Rotation and velocity dispersion in the stellar component of NGC 1316 (Fornax A)

Bosma, A.; Smith, R.M.; Wellington, K.J.

Mon. Not. R. astr. Soc. (1985) **212**, 301–307

Rotation and velocity dispersion in the stellar component of NGC 1316 (Fornax A)

A. Bosma★ *Sterrewacht, Postbus 9513, 2300 RA Leiden, The Netherlands and Mount Stromlo and Siding Spring Observatories, Private Bag, Woden PO, ACT 2606, Australia*

R. M. Smith *Mount Stromlo and Siding Spring Observatories, Private Bag, Woden PO, ACT 2606, Australia*

K. J. Wellington *CSIRO, Division of Radiophysics, PO Box 76, Epping, NSW 2121, Australia*

Accepted 1984 August 6. Received 1984 July 3; in original form 1983 September 12

Summary. Observations have been made of the stellar kinematics in NGC 1316, the galaxy associated with the strong radio source Fornax A. The galaxy is rotating rapidly about its photometric minor axis. A jump in the radial velocity of approximately $30\,\mathrm{km\,s^{-1}}$ is found along the major axis at the position of the first ripple in the luminosity profile. The velocity dispersion decreases from a nuclear value of $230\,\mathrm{km\,s^{-1}}$ to about $180\,\mathrm{km\,s^{-1}}$ at the first ripple, remaining approximately constant at larger radii. The data are consistent with the galaxy being an oblate spheroid flattened by rotation, with isotropic velocity dispersion. The presence of the radial velocity step agrees with the hypothesis that NGC 1316 is the result of at least one merger between a disc and an elliptical galaxy.

1 Introduction

NGC 1316, a 10.1 mag D galaxy near the edge of the Fornax cluster, is associated with the well-known radio source Fornax A. Schweizer (1980) attributes the peculiar morphology of the galaxy, with its tails and filaments in the outer parts and 'ripples', dust and gas in the inner parts, to the merging $\sim 10^9$ yr ago of several small disc galaxies with an elliptical galaxy. Radio observations of Fornax A by Ekers *et al.* (1983) using the Fleurs Synthesis Telescope showed that the bridge connecting the two extended lobes of radio emission does not pass through the nucleus of NGC 1316, a result which could lend further support to the view that this galaxy is a merger. VLA data by Geldzahler & Fomalont (1978), and also Fomalont (1981), show the existence of a bent jet-like source in the nuclear regions of the galaxy, a sign that the energy source there is still active.

★ Now at Observatoire de Marseille

† Now at Astronomy Centre, University of Sussex.

In this paper, we present new spectroscopic data on the stellar motions in the inner regions of NGC 1316. Already Schweizer (1980) has shown the existence of several ripples in the light distribution of the galaxy, a feature also found in numerous other elliptical galaxies as well (*cf.* Schweizer 1983). Plate 1 is a photograph of the central structure of NGC 1316 taken with the Anglo-Australian Telescope by B.A. Peterson and printed using the unsharp masking technique of Malin (Malin & Zealey 1979). This photograph clearly brings out the ripple structure, and the distribution of dust, in the inner parts of the galaxy. Stellar rotation data for the galaxy have been discussed previously by Searle (1965), Schweizer (1980) and Jenkins & Scheuer (1980). The first two papers presented evidence that the projected stellar rotation axis is close to the minor axis, nearly along the dust lane crossing the nucleus. Schweizer (1980) also finds evidence for a ring of gas along the minor axis, with rotation velocities of order of 350 km s^{-1}. Such gas rings have also been found in other peculiar ellipticals (e.g. NGC 5128, Graham 1979). Jenkins & Scheuer (1980) presented stellar rotation and velocity dispersion data out to about 20 arcsec radius, thus inside the radius of the innermost ripple, which has a diameter of $\sim 50 \times 30$ $arcsec^2$. Our new data extend out to 60 arcsec radius, hence we were able to get information across the ripple, and consequently we could check whether there are still peculiar motions associated with it.

2 Observations and reductions

We have observed NGC 1316 using the 3.9-m Anglo-Australian Telescope with the RGO spectrograph and the Image Photon Counting System (IPCS, Boksenberg & Burgess 1973). The IPCS was used in the two-dimensional mode which, with the extended memory, allowed us to use a format of 2000 wavelength channels by 50 spatial rows. The slitwidth was 190 μm, so that each pixel had a projected size of 1.3×4.45 $arcsec^2$ on the sky. A spectral range of 4600–5600 Å was chosen, to include Hβ, [O III], and the Mg b and Fe absorption lines. We observed at position angle 60°, corresponding to the major axis according to Schweizer (1980), for five times 1000 s exposures; each 1000 s was preceded and followed by exposures of a CuAr arc, and after that a sky reference frame was taken about 30 arcmin south of the galaxy with an exposure time of 500 s. We also observed a similar procedure for three times 1000 s exposures along a position angle of 141.°8, the apparent minor axis, from Plate 1. Spectra of several late-type stars were taken to provide a template spectrum for the Fourier analysis, and a spectrum of a white dwarf, L745–46A, Oke (1974), to provide a flux scale in case emission lines at Hβ and [O III] were detected. Finally, flat-field and twilight exposures were taken to correct for non-uniformities in the detector response. The seeing for most of the observations was ~ 3 arcsec.

A standard reduction procedure for IPCS observations was used (see e.g. Davies 1981). Each 1000 s frame was divided by the normalized flat-field and transformed to a log wavelength scale using the arc exposures. Drifts during the exposure were generally of the order of only 0.1 channels, and the fit to the arclines was accurate to ~ 0.15 Å. After the rebinning, the frames at each position angle were added. The night sky frames, similarly calibrated, were then subtracted with the appropriate weights; the resulting flux in the strong 5577 Å night sky line did not exceed 4 per cent of its initial value. The residual 5577 Å night sky line was replaced by the local continuum to minimize its effect in the Fourier techniques.

A template spectrum was produced from the observations of five late-type stars. In Table 1 we give details of these stars. The template spectrum matched the spectra of NGC 1316 rather closely. Radial velocities were determined using the Fourier methods described by Simkin (1974). At distances farther than 25 arcsec from the nucleus, rows were added to obtain sufficient signal-to-noise, with a total of at least 3×10^5 counts in each spectrum. Even

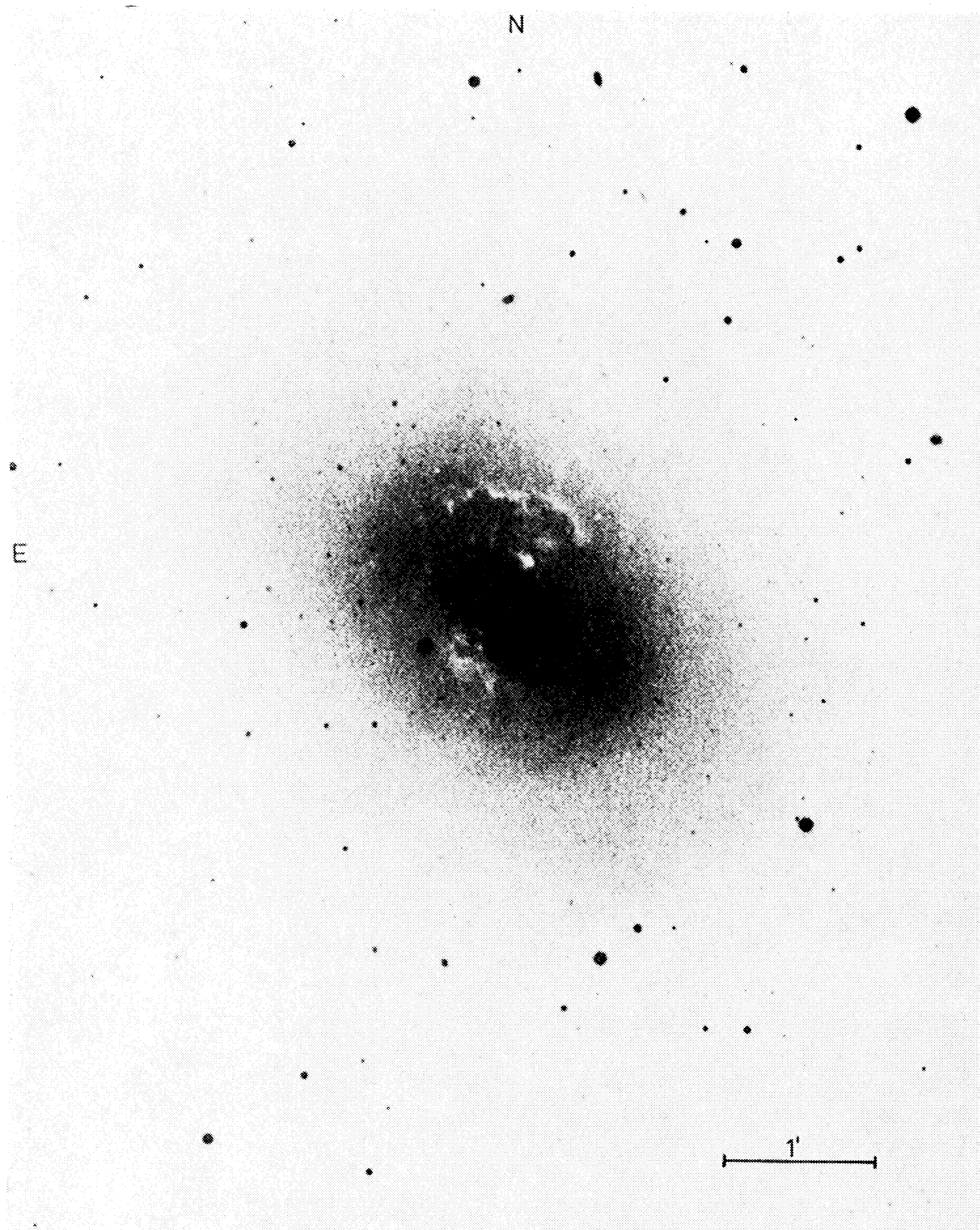

Plate 1. Photograph of the central structure of NGC 1316, obtained from a red plate (IIIaF+RG 610) taken by B. A. Peterson with the AAT prime focus camera, and printed by D. F. Malin using his unsharp masking technique.

[*facing page* 302]

Table 1. Radial velocity standards.

Standard star	Spectral type	Exposure time (s)	Velocity ($km\ s^{-1}$ wrt HD 222804)
HD 31871	K0 III	700	36
HD 215782	G5 III	1000	41
HD 219709	G8 III	700	2
HD 220465	G8 III	1300	29
HD 222804	K1 III	800	0

though the rotation curve is not flat in the outer parts, the gradient in radial velocity is small enough compared to the size of the errors to have little effect on the resulting velocities and velocity dispersions.

The velocity dispersions were calculated using both a parabola fit to the log power spectrum and, independently, a fit to the Fourier quotient in the manner described by Sargent *et al.* (1977). In the latter case, care was taken to exclude low-frequency variations due to the continuum. Both methods agreed within the errors although there is a small systematic difference in the results for the major axis. Errors in the parabola fit were estimated determing values for rotational velocities and velocity dispersions for 7 individual determinations from different parts of the spectrum. Although this does not take photon statistics into account, a reasonable representation of the errors is found.

3 Results

The rotational velocities and velocity dispersions for both position angles are listed in Table 2. The data for the two halves of the galaxies are in good agreement and have been folded and averaged around the nucleus in Fig. 1. The velocity dispersions along the major axis are those determined from the Fourier quotient technique as these most closely agreed in the nucleus

Table 2. Rotational velocities and velocity dispersions in NGC 1316.

Position angle 60°

Distance from nucleus (arcsec)	No. of rows averaged	NE-side		SW-side	
		V ($km\ s^{-1}$)	σ ($km\ s^{-1}$)	V ($km\ s^{-1}$)	σ ($km\ s^{-1}$)
2.23	1	13 ± 5	229 ± 22	3 ± 7	237 ± 27
6.68	1	51 ± 7	218 ± 30	44 ± 5	239 ± 22
11.13	1	89 ± 9	234 ± 19	58 ± 5	221 ± 11
15.58	1	88 ± 6	208 ± 19	72 ± 5	229 ± 31
22.25	2	84 ± 20	198 ± 29	84 ± 19	221 ± 32
26.70	2†	123 ± 11		132 ± 5	
31.15	2	90 ± 5	178 ± 18	112 ± 5	230 ± 27
42.28	3	117 ± 32	194 ± 41	97 ± 7	187 ± 27
57.85	4	115 ± 15	191 ± 18	115 ± 17	177 ± 26
76.76	4	133 ± 15		155 ± 13	167 ± 63
101.91	6	184 ± 48		139 ± 26	

Position angle 141°.8

Distance from nucleus (arcsec)	No. of rows averaged	SE-side		NW-side	
		V ($km\ s^{-1}$)	σ ($km\ s^{-1}$)	V ($km\ s^{-1}$)	σ ($km\ s^{-1}$)
0	1	0 ± 5	232 ± 13		
4.45	1	6 ± 7	215 ± 33	40 ± 13	212 ± 17
8.90	1	2 ± 10	193 ± 20	25 ± 18	168 ± 20
13.35	1	17 ± 18	175 ± 21	33 ± 19	196 ± 35
17.80	1	27 ± 24	197 ± 41	47 ± 8	160 ± 21
24.48	2	55 ± 15	166 ± 46	0 ± 21	169 ± 29
33.38	2	143 ± 64	146 ± 13	4 ± 28	184 ± 22
44.50	3	37 ± 9	140 ± 22	64 ± 11	189 ± 40
62.30	5	8 ± 16		33 ± 16	181 ± 34
91.23	8	69 ± 17	171 ± 15	11 ± 24	

† Note that an average has been taken over 2 rows, each of which are included in the preceding and following average. All velocity dispersions have been determined after shifting each row individually with its value for the rotation before averaging.

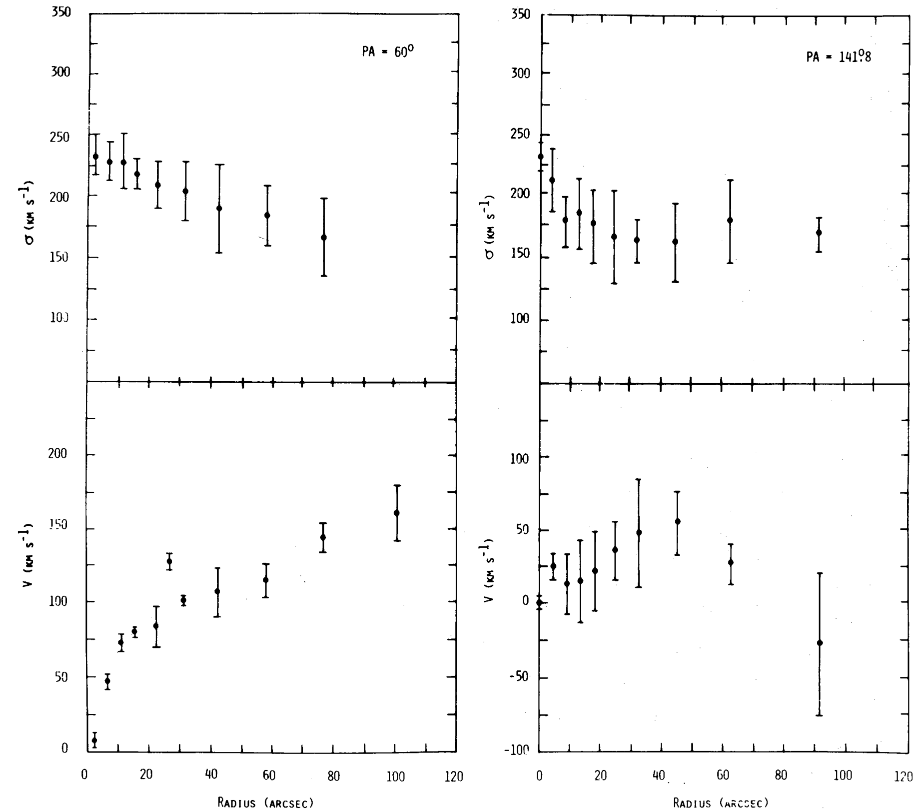

Figure 1. Rotation curve and velocity dispersion profiles for the two position angles measured. The data has been folded and averaged about the nucleus.

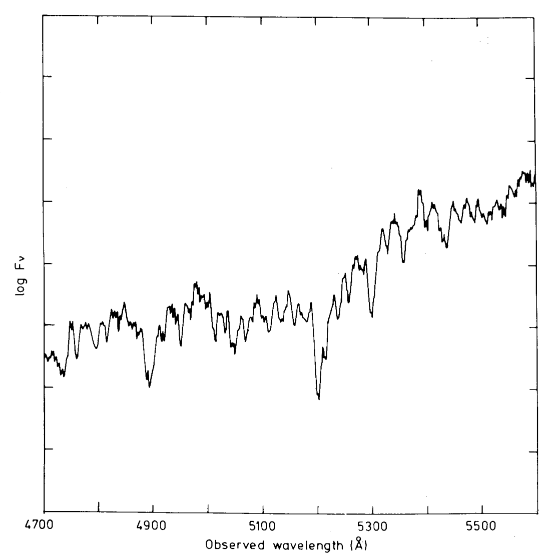

Figure 2. The central spectrum of NGC 1316, as obtained through an effective aperture of 1.3 × 13.4 arcsec^2 along position angle 141°8. The ordinate is in units of log F_ν, with F_ν in erg s^{-1} cm^{-2} Hz^{-1}, and rms from −24.56 (bottom) to −23.92 (top) with tick mark spacing of 0.16. The strongest absorption lines are Hβ at ~ 4900 Å and Mg *b* at ~ 5200 Å. No [O III] or Hβ emission is seen.

with the minor axis and that determined by Inglis (private communication). The shape of the dispersion curve is, however, identical using both methods. Each point is the mean of 7 individual determinations, and the error bars represent the dispersion around this ($\pm 1\sigma$).

Comparison with Plate 1 now shows the following results. Along position angle 60° the velocity dispersion drops from about 230 km s^{-1} in the centre to about 140 km s^{-1} beyond the position of the first ripple (which is at a radius of roughly 25 arcsec). At position angle 141°.8 the velocity dispersion drops very quickly from about 230 arcsec km s^{-1} at the centre to about 170 kms^{-1} at $\sim$15–20 arcsec distance from the nucleus, and stays roughly constant at larger distances. The radial velocities along pa = 60° increase smoothly to about 140 kms^{-1} at 60 arcsec radius, but at the position of the first ripple there is a jump in radial velocity of order 30 km s^{-1}. No such jump is seen at pa = 141°.8. Because of poor signal-to-noise ratio, we cannot say whether there are jumps in radial velocity at other 'ripples' in the luminosity distribution. (The ripples are of course local enhancements on a normal $r^{1/4}$-law distribution of light.)

Our results can be compared with those given by Jenkins & Scheuer (1980) who have data at position angles 40° and 110°. The rotation velocities are comparable when orientation parameters are taken into account. In fact, using the available data, if we solve for circular motion in a disc, we derive a position angle of the line of nodes of 50° ± 5° and an inclination angle of 54° ± 5°.

Fig. 2 shows the central spectrum of NGC 1316 obtained by summing the three central rows of the minor axis data. No [O III] or Hβ emission is seen, the latter being present strongly in absorption.

4 Discussion

4.1 COMPARISON WITH OTHER GALAXIES

From our measurement we derive a V_m/σ_0, with V_m the maximum observed rotational velocity and σ_0 the central velocity dispersion, of order 0.6–0.7, while from Plate 1 we estimate an ellipticity of 0.2–0.3. This can be compared with data for other ellipticals galaxies which are associated with radio sources. In Table 3 we have collected data for a number of galaxies from Davies *et al.* (1983) and Jenkins & Scheuer (1980) and Smith *et al.*

Table 3. Comparison of NGC 1316 with other radio ellipticals.

Galaxy	Ellipticity	V_m (km s^{-1})	σ_0 (km s^{-1})	M_B^{UH}	V_m/σ_0	$(V_m/\sigma_0)^*$	Ref
NGC 315	0.31	≤30	314 ± 26	− 23.08	≤0.10	≤0.15	1
NGC 1052	0.31	96 ± 5	245 ± 7	− 20.87	0.46	0.69	1
NGC 3557	0.32	178 ± 20	222 ± 16	− 22.26	0.70	1.02	1
NGC 4278	0.07	50 ± 10	243 ± 8	− 20.30	0.20	0.73	1
NGC 4374	0.10	≤38	298 ± 6	− 21.24	≤0.13	≤0.38	1
NGC 4486	0.14	≤20	336 ± 7	− 21.99	≤0.07	≤0.17	1
NGC 7626	0.17	≤30	270 ± 14	− 22.23	≤0.09	≤0.20	1
IC 4926	0.10	64 ± 12	300 ± 9	− 22.94	0.22	0.66	1
NGC 741	0.3	300 ± 30	300 ± 30	− 22.08	1.00	1.53	2
NGC 5090	0.15	70 ± 10	271 ± 10	− 21.40	0.26	0.60	3
NGC 1316	0.2 − 0.3	150 ± 10	233 ± 10	− 22.90	0.64	1.28 − 0.98	4

References

1. Davis *et al.* (1983).
2. Jenkins and Scheuer (1980).
3. Smith *et al.* (1984, in preparation).
4. This paper.

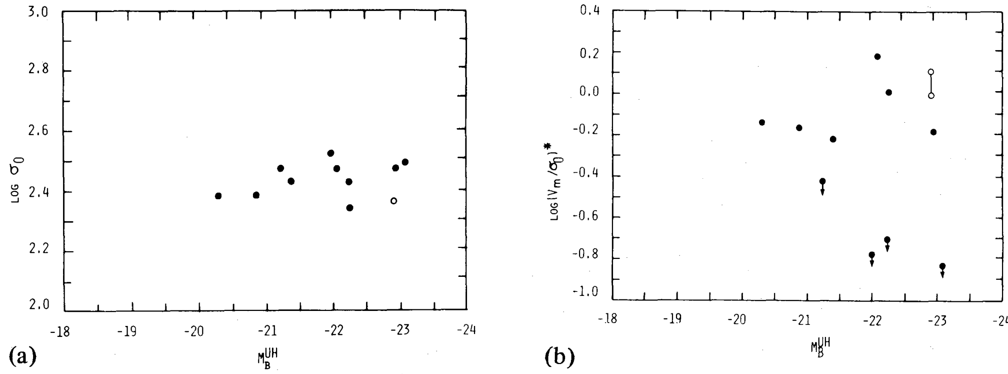

Figure 3. (a) Logarithm of velocity dispersion plotted against absolute B magnitude for radio ellipticals. NCG 1316 is represented by the open circle. (b) The ratio of observed V/σ versus that expected if the galaxies were oblate spheroids flattened by rotation, denoted $(V_m/\sigma)^*$, plotted against absolute B magnitude for radio galaxies. The limits set by the ellipticity of NGC 1316 are shown by open circles.

(1984, in preparation). In column 5 of that table we give the intrinsic blue luminosity based on $H_0 = 50\,\mathrm{km\,s^{-1}\,Mpc^{-1}}$ and assuming a uniform Hubble flow. In column 7 we give the ratio of observed V_m/σ_0 with that expected if the galaxy was an oblate spheroid whose flattening is due to rotation, denoted as $(V_m/\sigma_0)^*$ (*cf.* Binney 1978, and Davies *et al.* 1983). In Fig. 3a and b we give a graphical comparison of NGC 1316 with the other galaxies in the form of a classic log σ_0 versus $-M_B^{\mathrm{UH}}$ diagram, and a diagram of log $(V_m/\sigma_0)^*$ versus $-M_B^{\mathrm{UH}}$.

From these diagrams, and a comparison with a similar diagrams for normal ellipticals in e.g. Illingworth (1983), we can see that NGC 1316 is a relatively fast rotation compared to normal bright elliptical galaxies. Also its central velocity dispersion is relatively low compared to other galaxies of the same absolute magnitude. NGC 1316 is, however, not truly exceptional, since there are several other galaxies with similar properties. Yet Fig. 3 and Table 3 show that not all radio galaxies are fast rotators. Perhaps there is a tendency for the slow rotators to lie in a cluster environment, since the 4 galaxies with upper limits for V_m/σ_0 all happen to lie in clusters, while the others are in small groups. More observational work needs to be done to see whether there is a correlation between the dynamical properties of elliptical galaxies and the occurence of the radio source phenomenon.

4.2 IMPLICATIONS OF THE MERGER SCENARIO

Our finding of a velocity jump across the first ripple at position angle 60° is interesting in view of the proposal by Quinn (1984) to explain the ripples and shells around some elliptical galaxies, discussed by Malin & Carter (1980) and Schweizer (1983), as the result of a merger of an elliptical galaxy and a disc galaxy. He argues that the shells and ripples reflect the various stages of the wrapping of the disc around the centre of the potential. One would then expect small peculiar velocities to be associated with the ripples, and these velocities to be directed away from the nucleus. The expected magnitude of the velocities and their direction is in qualitative agreement with our results (*cf.* Quinn 1984), but it should be noted that no attempt has been made so far to model NGC 1316 itself.

The other main result, i.e. that the velocity dispersion and the rotational velocities of the stars become roughly equal at $\sim$1 arcmin radius, implies that NGC 1316 has higher stellar rotational velocities than is usual for giant elliptical galaxies. Since the dispersion profiles, when adjusted for the effect of the axial ratio of 0.7, look alike along both position angles the velocity distribution is nearly isotropic. Not enough is known about the dynamics of merging an elliptical and a disc galaxy to say whether this fact constitutes a significant constraint.

5 Conclusions

Our observations of the stellar kinematics in NGC 1316 (Fornax A) revealed the presence (at the 2–3σ level) of a radial velocity jump across the innermost ripple in the light distribution of this galaxy. This is in agreement with the merger scenario described by Schweizer (1980, 1983), and theoretical expectations of a disc/elliptical merger as considered by Quinn (1984).

We also find that NGC 1316 has a relatively high V_m/σ_0, which arises partly from its low value of σ in view of its luminosity. Our data are consistent with the galaxy being an oblate spheroid with isotropic velocity distribution and flattened by rotation, although its peculiarities may not justify comparison with such a model.

Acknowledgments

We would like to thank ATAC for the allocation of telescope time. We are also very grateful to Dave Malin for providing the print for Plate 1, with the kind permission of Bruce Peterson. Dave Carter provided the Fourier quotient programs, together with many helpful discussions. RMS acknowledges receipt of an ANU postgraduate research award.

References

Binney, J., 1978. *Mon. Not. R. astr. Soc.*, **183**, 501.

Boksenberg, A. & Burgess, D. E., 1973. *Astronomical Observations with Television-Type Sensors*, p. 21, eds Glaspey, J. W. & Walker, G. A. H., University of British Columbia, Vancouver.

Davies, R. L., 1981. *Mon. Not. R. astr. Soc.*, **194**, 879.

Davies, R. L., Efstathiou, G., Fall, S. M., Illingworth, G. & Schechter, P. L., 1983. *Astrophys. J.*, **266**, 41.

Ekers, R. D., Goss, W. M., Bosma, A., Wellington, K. J., Smith, R. M. & Schweizer, F., 1983. *Astr. Astrophys.* **127**, 361.

Fomalont, E. B., 1981. *Origin of Cosmic Rays, IAU Symp. No. 94*, p. 111, eds Setti, G., Spada, G. & Wolfendale, A. W., Reidel, Dordrecht, Holland.

Geldzahler, B. J. & Fomalont, E. B., 1978. *Astr. J.*, **83**, 1047.

Graham, J. A., 1979. *Astrophys. J.*, **232**, 60.

Illingworth, G., 1983. *Kinematics and Dynamics of Galaxies, IAU Symp. No. 100*, p. 257, ed. Athanassoula, E., Reidel, Dordrecht, Holland.

Jenkins, C. R. & Scheuer, P. A. G., 1980. *Mon. Not. R astr. Soc.*, **192**, 595.

Malin, D. F. & Carter, D., 1980. *Nature*, **285**, 643.

Malin, D. F. & Zealey, W., 1979. *Sky Telesc.* **57**, 354.

Oke, J. B., 1974. *Astrophys. J. Suppl.*, **27**, 21.

Quinn, P. J., 1984. *Astrophys. J.*, **279**, 596.

Sargent, W. L. W., Schechter, P. K., Boksenberg, A. & Shortridge, K., 1977. *Astrophys. J.*, **212**, 326.

Schweizer, F., 1980. *Astrophys. J.*, **237**, 303.

Schweizer, F., 1983. *Kinematics and Dynamics of Galaxies, IAU Symp. No. 100*, p. 319, ed. Athanassoula, E. Reidel, Dordrecht, Holland.

Searle, L., 1965. *Nature*, **207**, 1282.

Simkin, S. M., 1974. *Astr. Astrophys.*, **31**, 129.